

See discussions, stats, and author profiles for this publication at: <https://www.researchgate.net/publication/41409870>

Insight into the mechanism of action of plakortins, simple 1,2-dioxane antimalarials

ARTICLE in ORGANIC & BIOMOLECULAR CHEMISTRY · FEBRUARY 2010

Impact Factor: 3.56 · DOI: 10.1039/b918600j · Source: PubMed

CITATIONS

19

READS

33

10 AUTHORS, INCLUDING:



Ernesto Fattorusso

University of Naples Federico II

390 PUBLICATIONS 8,392 CITATIONS

SEE PROFILE



Vincenzo Barone

Scuola Normale Superiore di Pisa

771 PUBLICATIONS 43,239 CITATIONS

SEE PROFILE



Paola Cimino

Università degli Studi di Salerno

41 PUBLICATIONS 893 CITATIONS

SEE PROFILE



Caterina Fattorusso

University of Naples Federico II

89 PUBLICATIONS 1,975 CITATIONS

SEE PROFILE

Insight into the mechanism of action of plakortins, simple 1,2-dioxane antimalarials†

Orazio Tagliatela-Scafati,^a Ernesto Fattorusso,^a Adriana Romano,^a Fernando Scala,^a Vincenzo Barone,^{b,c} Paola Cimino,^{c,d} Emiliano Stendardo,^e Bruno Catalanotti,^a Marco Persico^a and Caterina Fattorusso^{*a}

Received 8th September 2009, Accepted 7th November 2009

First published as an Advance Article on the web 16th December 2009

DOI: 10.1039/b918600j

A multidisciplinary approach, based on molecular dynamics/mechanics, *ab initio* calculations, dynamic docking studies, and chemical reactions, has been employed to gain insight into the mechanism of the antimalarial action of plakortin and dihydroplakortin, simple 1,2-dioxanes isolated from the sponge *Plakortis simplex*. Our results show that these molecules, after interaction of the endoperoxide bond with Fe(II), likely coming from the heme molecule, give rise to the formation of an oxygen radical, followed by rearrangement to give a carbon radical centered on the “western” alkyl side-chain. The carbon radicals generated on the side-chain, amenable for intermolecular reactions, should represent the toxic intermediates responsible for subsequent reactions leading to plasmodium death. The minimal structural requirements necessary for the activity of this class of antimalarial agents have been identified and discussed throughout the paper.

1. Introduction

Malaria, an infectious disease caused by protozoans belonging to the genus *Plasmodium*, is still a common cause of death in Africa and in other poor tropical countries (each year, 300–500 million people become ill with malaria and 1–3 million die).¹ Since malaria is a disease of worldwide implications, and almost half of the world's population is currently at risk of malaria infection, combating malaria is one of the highest priority programs of the WHO.² A worrisome increase in the number of fatal cases has been registered in recent years and it is principally due to the diffusion of multi-drug resistant strains of *Plasmodium*, making less effective the limited arsenal of available drugs. Moreover, the available chemical weapons to treat malaria cases are sadly based on very old molecules, such as the chloroquine (CQ) analogues. Although the association of these molecules with analogues of artemisinin (**1**) (Fig. 1), a natural endoperoxide derivative active against many resistant strains,³ is giving some good results, the therapeutic choices are still too limited for the large and poor malaria market. Therefore, there is an urgent need of new and economically affordable antimalarial drugs.

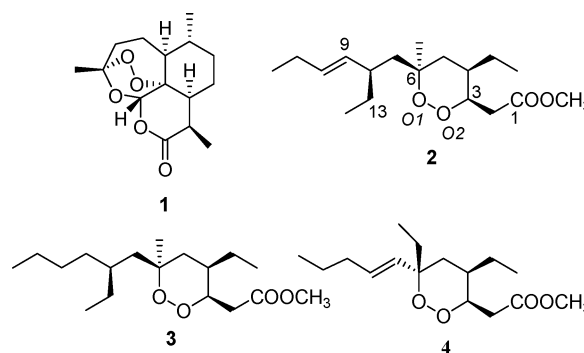


Fig. 1 Reference and title compounds: artemisinin (**1**), plakortin (**2**), dihydroplakortin (**3**) and plakortide K (**4**).

In this context, several research groups are currently engaged in the isolation of new antimalarial compounds from terrestrial plants and marine organisms to be used as lead compounds for the development of effective and, possibly, cheap drugs.⁴ We reported few years ago that plakortin (**2**) (Fig. 1), a simple endoperoxide-containing polyketide isolated in high yields from the Caribbean sponge *Plakortis simplex*,⁵ possesses significant *in vitro* antimalarial activity on CQ-resistant strains of *Plasmodium falciparum* (Table 1).⁶ Dihydroplakortin (**3**) (Fig. 1), 3-epiplakortin and plakortide Q, very minor analogues of plakortin extracted from the same sponge, proved to be almost equally active.⁷ In addition, we have recently prepared a series of semi-synthetic derivatives of plakortin in order to gain insights into the structural requirements of these simple 1,2-dioxanes for exhibiting antimalarial activity. The obtained results confirmed the crucial role of the endoperoxide functionality (the plakortin diol is completely inactive) and revealed conformation-dependent features critical for antimalarial activity.⁸

The knowledge of further details on the mechanism of action at the molecular level constituted an issue of key importance to continue our investigation on the antimalarial activity of

^aDipartimento di Chimica delle Sostanze Naturali, Università di Napoli “Federico II”, Via D. Montesano 49, I-80131 Napoli, Italy. E-mail: cfattorus@unina.it; Fax: +39-081-678552; Tel: +39-081-678544

^bScuola Normale Superiore di Pisa, Piazza dei Cavalieri 7, I-56126 Pisa, Italy

^cIstituto per i Processi Chimico-Fisici del Consiglio Nazionale delle Ricerche (IPCF-CNR) Area delle Ricerche del CNR, via Moruzzi 1, I-56126 Pisa, Italy

^dDipartimento di Scienze Farmaceutiche, Università di Salerno, Università di Salerno, Via Ponte don Melillo, 84084 Fisciano-Salerno, Italy

^eDipartimento di Chimica, Università di Napoli “Federico II”, Complesso Universitario Monte S. Angelo, via Cintia, I-80126 Napoli, Italy

† Electronic supplementary information (ESI) available: HPLC traces for the separation of **5a/5b** and **6a/6b** and ¹H NMR spectra of compounds **5a** and **6a**. See DOI: 10.1039/b918600j

Table 1 *In vitro* antimalarial activity of compounds **1–4** against D10 (CQ-S) and W2 (CQ-R) strains of *Plasmodium falciparum*

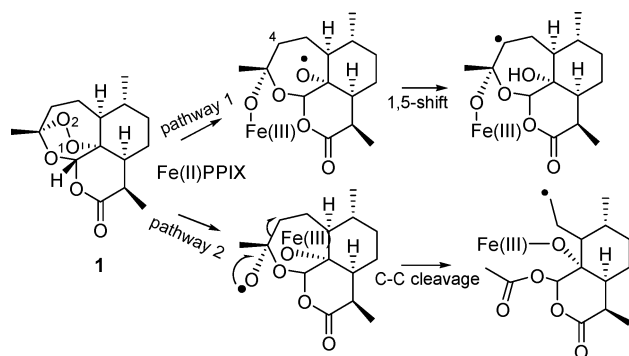
	D10 IC ₅₀ /μM	W2 IC ₅₀ /μM
Plakortin (2) ^a	0.87 ± 0.35	0.39 ± 0.13
Dihydroplakortin (3) ^a	0.90 ± 0.56	0.43 ± 0.16
Plakortide K (4) ^b	Not available	>2
Artemisinin (1) ^a	0.013 ± 0.004	0.009 ± 0.005

^a Data taken from ref. 8 ^b Data taken from ref. 18

plakortin derivatives. Indeed, a more detailed comprehension of the mechanism of the action of plakortins could pave the way for the development of totally synthetic simplified derivatives containing only the essential pharmacophoric portion of the plakortin scaffold.

Despite the large use of artemisinin, the exact molecular mechanism underlying its biological activity, and that of related antimalarial endoperoxides, is still a matter of debate.⁹ Nevertheless, the ability of these molecules to interact with Fe(II)-heme and to produce oxidative stress hallmarks in the plasmodium and in the infected host cells has been proved.^{9,10} The reaction of endoperoxides with Fe(II) involves a one-electron reduction leading to the cleavage of the oxygen–oxygen linkage with the consequent formation of an oxygen anion [bound to Fe(III)] and of an oxygen free radical. Two possible evolutions of the generated oxygen radical have been postulated for artemisinin (Scheme 1). In pathway 1, the oxygen O1 free radical evolves through an intramolecular 1,5-H shift leading to a secondary free radical at C4. Alternatively, in pathway 2, the oxygen O2 free radical evolves through a homolytic cleavage of the C3–C4 bond resulting in the formation of a primary C4 free radical, the driving force being the acquisition of thermodynamic stability by formation of the acetate group.⁹ Experimental data¹¹ and theoretical studies¹² show controversial results on the more relevant pathway for antimalarial activity. Anyway, reported structure–activity relationship (SAR) studies on artemisinin,¹³ as well as on other endoperoxide derivatives,¹⁴ failed to relate *in vitro* antimalarial activity with a mechanism of action principally based on reaction pathway 2. In addition, the lack of antimalarial activity of artemisinin analogues with α-oriented substituents at C4 can be related to their inability to undergo the intramolecular 1,5 H-shift (pathway 1).¹³

The crucial role of the endoperoxide function and of 1,2-dioxane ring conformation that we have demonstrated for **2**,⁸



Scheme 1 Schematic representation of the artemisinin postulated mechanism of action.

together with the lack of stereoselectivity in its antimalarial mechanism of action (3-epiplakortin showed the same activity as **2**⁷), strongly indicated that plakortin, similarly to artemisinin, does not interact with a specific protein target but rather with a Fe(II) ion, most likely the heme iron derived from hemoglobin digestion.¹⁵ Our previous conclusion that the antimalarial activity of plakortin and its analogues is strongly affected by conformational parameters⁸ prompted us to speculate on a through-space reaction pathway for the formation of reactive species responsible for plasmodium death. Starting from this assumption, we carried out our investigation on compounds **2** and **3** (Fig. 1), two related compounds which showed comparable antimalarial activity (Table 1). The aim was to enlighten, for both these compounds, the steps following the reductive activation of the oxygen–oxygen bond by Fe(II) species and yielding to the death of the parasite. Our approach followed two independent methods based on computational analysis and chemical evidence and represents the first investigation on the mechanism of action of non-peroxyketal simple dioxane antimalarials.

2. Results

2.1 Computational studies

In order to sample plakortin and dihydroplakortin conformational space we performed an integrated computational analysis, following a protocol that combines molecular dynamics and mechanics, as well as semi-empirical (PM6) quantum-mechanical (QM) calculations (see the Experimental section). The generated conformers for both **2** and **3** were grouped into families on the basis of 1,2-dioxane ring conformation and potential energy values (*i.e.*, Δ*E* from the global minimum) and occurrence rates were calculated. Obtained results (Fig. 2, Table 2) indicated that ‘Chair A’ is by far the most representative 1,2-dioxane ring conformational family for both plakortin and dihydroplakortin.

Subsequent calculations were performed on the basis of the hypothesized reaction pathway responsible for antimalarial activity.

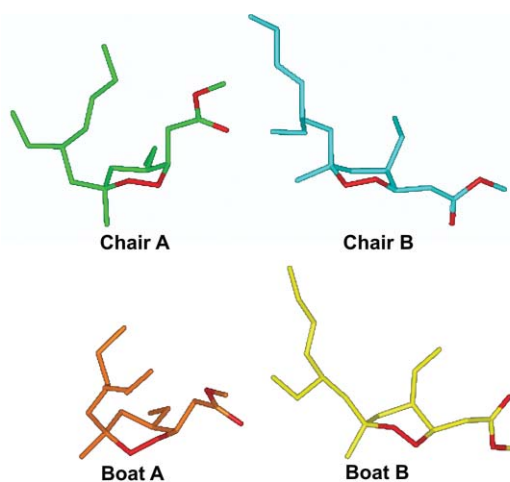


Fig. 2 Lowest energy minima of each 1,2-dioxane ring conformation family of plakortin. Carbons are in green (Chair A), cyan (Chair B), orange (Boat A) and yellow (Boat B); oxygens are in red. All hydrogens are omitted for clarity. Parallel families were found for dihydroplakortin.

Table 2 Occurrence rate of 1,2-dioxane ring conformations considering Molecular Mechanic (MM) and PM6 conformers within 5 Kcal mol⁻¹ from the global minimum

	Plakortin (%)		Dihydroplakortin (%)	
	MM	PM6	MM	PM6
Chair A	92	82	93	84
Chair B	7	6	7	8
Boat A	1	11	0	7
Boat B	0	1	0	1

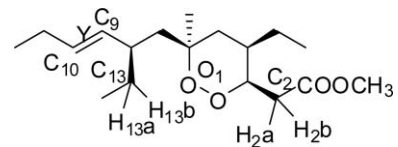
The first reaction step, the activation step, involves a one-electron reduction by heme Fe(II), thus leading to the cleavage of the endoperoxide bond, through a dissociative electron transfer (DET) mechanism.^{16,17} Within this step, an oxygen anion [bound to Fe(III)] and an oxygen free radical are produced. Since the endoperoxide linkage has two oxygen atoms exposed to the heme iron (named O1 and O2 for **2**, see Fig. 1), *ab initio* calculations were performed in order to investigate the alternative formation of O1 and O2 radicals. A hydrogen atom in place of Fe(III) was introduced to counterbalance the negative charge of the oxygen anion. Since the calculated occurrence rate of 1,2-dioxane ring families of conformers indicated Chair A as the most representative family (>80%, Table 2), we focused our *ab initio* calculations on Chair A PM6 low energy conformers (*i.e.*, within 5 kcal mol⁻¹ of the global minimum). Three different orientations of the introduced hydroxyl hydrogen were generated (rotating O1–C6 or O2–C3 bonds by increments of 120°) and the resulting conformations were considered as starting geometries for *ab initio* optimization. Results, reported in Table 3, indicated unambiguously a higher stability for the O1 radical. Since the energies of the transition states for the two alternative homolytic cleavage reactions are likely to be in proportion to those of the corresponding products (oxygen radicals), we can assume that the formation of the O1 radical is kinetically preferred both for **2** and **3**. Accordingly, we continued our investigation with the assumption that the radical is preferentially formed on O1.

Table 3 *Ab initio* calculated relative stability of O1 and O2 radicals

		ΔE^d /Kcal mol ⁻¹	ΔE^e
Plakortin (2)			
CNF_50 ^a	RadO1 ^b	-73.704	0
	RadO2 ^b	-69.378	4.326
CNF_152 ^a	RadO1 ^b	-72.865	0
	RadO2 ^b	-69.534	3.331
CNF_365 ^a	RadO1 ^b	-72.302	0
	RadO2 ^b	-69.161	3.141
Dihydroplakortin (3)			
CNF_132 ^a	RadO1 ^c	-71.314	0
	RadO2 ^b	-70.408	0.906
CNF_173 ^a	RadO1 ^b	-72.104	0
	RadO2 ^b	-69.354	2.750

^a Chair A low energy PM6 conformer used as starting geometry; ^b Lowest energy O1 and O2 radical forms, presenting a hydrogen bond between the oxygen radical and the hydroxyl hydrogen; ^c Lowest energy O1 radical form, presenting a hydrogen bond among the carbonyl oxygen, O1, and O2–H; ^d $\Delta E = E_{\text{O radical}} - (E_{\text{neutral}} + E_{\text{H radical}})$; ^e Energy difference calculated with respect to the most stable oxygen radical for each conformer.

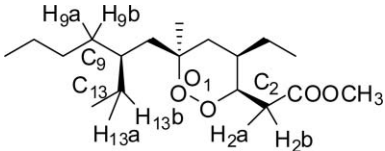
Table 4 Molecular Mechanics (MM) and PM6 conformers of plakortin owning interatomic distances suitable for a radical shift from O1 (≤ 3 Å). Involved atoms, occurrence rates, 1,2-dioxane ring conformations

					
CNF ^a (%) Chair A ^b (%) Chair B ^b (%) Boat A ^b (%) Boat B ^b (%)					
MM					
Y ^c	9	100	0	0	0
C9	17	100	0	0	0
H13a	16	89	11	0	0
H13b	6	86	14	0	0
H2a	70	100	0	0	0
H2b	11	100	0	0	0
PM6					
C10	6	100	0	0	0
Y ^c	7	100	0	0	0
C9	18	100	0	0	0
H13a	18	89	5	6	0
H13b	6	100	0	0	0
H2a	76	100	0	0	0
H2b	55	97	0	0	3

^a Rate of conformers within 5 Kcal mol⁻¹ from the global minimum owning a distance between the involved atom and O1 ≤ 3 Å; ^b Rate of conformers belonging to this family; ^c Double bond centroid.

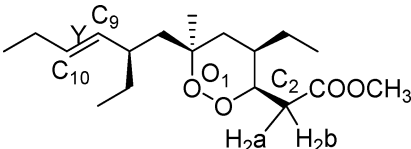
We next evaluated the distance between the endoperoxide oxygen O1 and the possible partners for an intramolecular radical shift through an analysis of conformational search results. Since for both compounds, more than one possible reaction partner (Tables 4 and 5) was found, we deepened this investigation. To this end, the lowest energy PM6 conformers possessing intramolecular distances suitable to allow an intramolecular radical shift from O1 (≤ 3 Å)⁹ were subjected to *ab initio* calculations in the neutral, as well as, in the O1 radical form, and, finally, intramolecular distances were checked on the obtained conformations (Fig. 3). The evaluation of these results (Tables 6 and 7) suggested the double bond of plakortin and the methylene hydrogens at C13 of dihydroplakortin as the most likely partners for interaction with the O1 radical. Indeed, our calculations suggested that, as a consequence of the conformational rearrangement following the cleavage of the endoperoxide bond, in both compounds, the O1-centered radical approached the “western” alkyl side-chain [*i.e.*, the double bond in **2** and C(13)H in **3**, respectively] shrinking from the ester side-chain [*i.e.*, C(2)H]. This conformational shift is in agreement with the previously explored SARs on 1,2-dioxane derivatives that indicated a negligible role for the “eastern” ester side-chain.⁸ On the other hand, the role of the “western” alkyl side-chain for the antimalarial activity of 1,2-dioxanes is well highlighted by plakortin **4** (Fig. 1). This compound, obtained from *Plakortia* sp.,¹⁸ proved to be completely inactive as antimalarial agent (Table 1), in spite of its similarity to plakortin, including an identical ester side-chain (Fig. 1). In agreement with our results, the lack of activity should be ascribed to the presence of the $\Delta^{7,8}$ *trans* double bond, whose geometry prevents the location of a reaction partner on the western side chain at a distance suitable for the intramolecular shift.

Table 5 Molecular Mechanic (MM) and PM6 conformers of dihydroplakortin owning interatomic distances suitable for a radical shift from O1 (≤ 3 Å). Involved atoms, occurrence rates, 1,2-dioxane ring conformations

					
Involved atom	CNF ^a (%)	Chair A ^b (%)	Chair B ^b (%)	Boat A ^b (%)	% Boat B ^b
MM					
H13a	28	89	11	0	0
H13b	16	87	13	0	0
H9a	15	93	7	0	0
H9b	24	96	4	0	0
H2a	65	100	0	0	0
H2b	11	100	0	0	0
PM6					
H13a	20	86	11	3	0
H13b	9	100	0	0	0
H9a	7	100	0	0	0
H9b	15	93	7	0	0
H2a	76	99	0	0	1
H2b	42	97	0	0	0

^a Rate of conformers within 5 Kcal mol⁻¹ from the global minimum owning a distance between the involved atom and O1 ≤ 3 Å; ^b Rate of conformers belonging to this family.

Table 6 Plakortin: Interatomic distances between O1 and possible intramolecular radical shift partners calculated on the neutral and O1 radical forms of *ab initio* conformers and on bioactive conformation

						
		Distances/Å				
Plakortin		O1-C10	O1-Y	O1-C9	O1-H2a	O1-H2b
CNF_1	Neutral	3.78	3.33	2.97	2.49	3.78
	Radical ^a	2.94	2.63	2.47	2.99	4.44
CNF_2	Neutral	3.07	3.17	3.39	2.48	3.78
	Radical ^a	2.60	2.65	2.87	2.80	4.29
BC ^b	Neutral	3.98	3.47	3.04	2.93	2.70

^a Lowest energy O1 radical form, presenting a hydrogen bond between O1 and O2-H; ^b Putative plakortin bioactive conformation.

In order to refine the structural features underlying the anti-malarial activity of **2** and **3**, all *ab initio* conformers reported in Fig. 3 were used as starting geometries for dynamic docking studies in complex with heme (Fe(II)-FPIX). To ensure that the results obtained were independent from the starting geometries, during these docking simulations, the system (ligand and heme) was left free to move and a Monte Carlo conformational search was applied considering all the rotating bonds of the ligand; moreover, a Simulated Annealing procedure was performed (see the Experimental section). Interestingly, both plakortin and dihydroplakortin conformations resulting from docking studies shared crucial structural parameters for the hypothesized carbon

Table 7 Dihydroplakortin: Interatomic distances between O1 and possible intramolecular radical shift partners calculated on the neutral and O1 radical forms of *ab initio* conformers and on putative bioactive conformation

		Distances/Å			
Dihydroplakortin		O1-H13a	O1-H13b	O1-H2a	O1-H2b
CNF_1	Neutral	2.25	3.74	3.89	3.31
	Radical ^a	2.20	3.80	4.53	4.61
CNF_2	Neutral	2.32	3.25	2.78	2.75
	Radical ^b	2.15	3.03	3.71	2.37
BC ^c	Neutral	2.47	3.77	3.95	3.44

^a Lowest energy O1 radical form, presenting a hydrogen bond among the carbonyl oxygen, O1, and O2-H; ^b Lowest energy O1 radical form, presenting a hydrogen bond between O1 and O2-H; ^c Putative dihydroplakortin bioactive conformation.

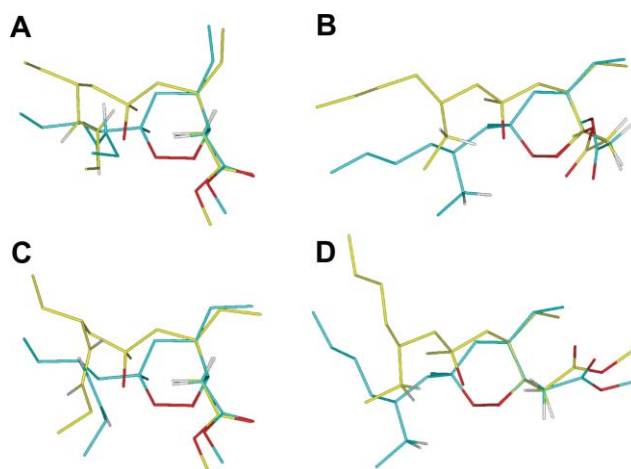


Fig. 3 (A–D): comparison between *ab initio* conformers in the neutral (cyan) and O1 radical form (yellow) of plakortin (CNF_1 (A) and CNF_2 (C)) and dihydroplakortin (CNF_1 (B) and CNF_2 (D)). The molecules are colored by atom type (O = red and H = white). Hydrogens are omitted for sake of clarity, with the exception of those involved as possible partners in a “through-space” intramolecular radical shift.

radical formation with CNF_1 *ab initio* conformers (Fig. 4; Table 6 and 7). As depicted in Fig. 4C, D, in agreement with previous results, both plakortin and dihydroplakortin interacted with the heme adopting the Chair A conformation of the 1,2-dioxane ring and positioning the “western” alkyl side-chain in proximity to O1. In particular, in the case of plakortin, the closest atom was the first carbon of the double bond (C9), while, in the case of dihydroplakortin the closest atoms were the hydrogen atoms attached at C13. As for the possible interaction of the O1 radical with C2 methylene hydrogens, docking studies revealed a different behavior for plakortin and dihydroplakortin. In the latter compound, an interaction of the ester carbonyl oxygen with heme iron pushes C2 hydrogen atoms far from O1. In contrast, in the case of plakortin, the proximity of the O1 radical and C2

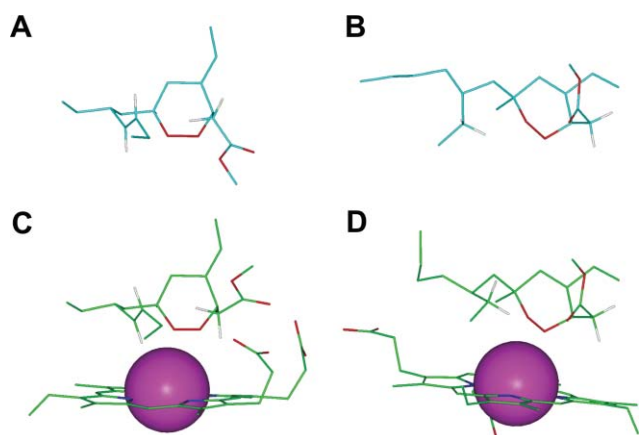


Fig. 4 (A–B): *Ab initio* conformers of plakortin (A) and dihydroplakortin (B). (C–D): docking results of plakortin (C) and dihydroplakortin (D) in complex with heme. The molecules are colored by atom type (C = cyan and green for *ab initio* and docking conformers, respectively; O = red; N = blue; Fe = magenta and H = white). Iron atoms vdW volumes are shown. Hydrogens are omitted for sake of clarity, with the exception of those involved as possible partners in a “through-space” intramolecular radical shift.

hydrogen atoms cannot be excluded, since interaction between the

heme iron and the carbonyl oxygen is prevented by unfavorable steric contacts occurring between the two (*i.e.*, ester and “western”) alkyl side-chains. However, the greater reactivity of the double bond in an electron transfer reaction must be taken into account and, in place of the conformational preference, as in the case of dihydroplakortin, could be the factor driving the rearrangement of O1-centered radical toward the “western” alkyl side-chain. This hypothesis is supported by the intramolecular distances calculated on *ab initio* conformers of plakortin, which evidenced a strong interaction between the double bond and O1 when the radical is formed (compare these distances between neutral and radical forms in Table 6).

Taken together, all the computational outcomes indicated the structures reported in Fig. 4 as putative plakortin and dihydroplakortin bioactive conformations, being able to undergo: 1) a one-electron reduction reaction of the endoperoxide bond by heme Fe(II) through a DET mechanism, leading to the formation of an oxygen radical at O1; 2) a subsequent through-space one

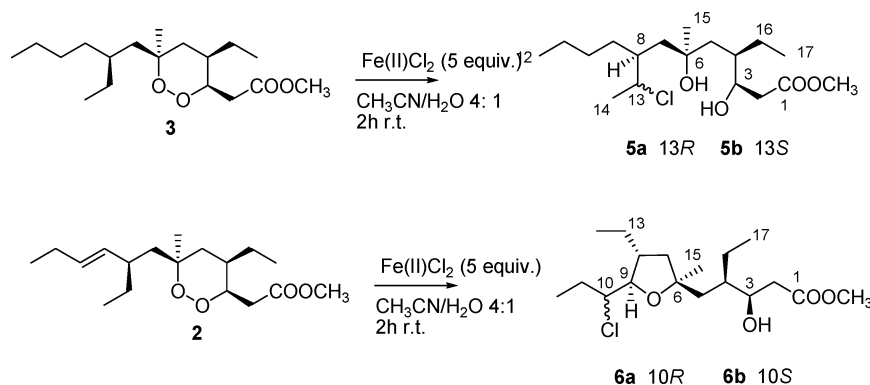
electron reaction between O1 radical and the double bond (C9), in the case of plakortin, and between O1 radical and an ethyl chain (C13) hydrogen, in the case of dihydroplakortin. The generated carbon radicals could represent, according to the hypothesized mechanism of action, toxic intermediates responsible for subsequent reactions leading to plasmodium death.

2.2 Reaction with Fe(II) chloride

To check experimentally the results of computational calculations, we decided to utilize the model Fe(II)-induced reduction of the endoperoxide bond¹⁹ and to analyze the behavior of both **3** and **2** by detailed characterization of their degradation products. Among the possible experimental models, we preferred the use of (inorganic) salts of Fe(II) in aqueous solution due to the efficiency and reproducibility of the reaction.²⁰ Data available in the literature for artemisinin and other endoperoxide antimalarials are almost exclusively based on the use of Fe(II) chloride, sulfate, or gluconate.²¹ A recently appeared investigation has established that Fe(II) chloride is very efficient in triggering artemisinin endoperoxide bond cleavage and subsequent intramolecular rearrangement.²⁰

Thus, **3** was allowed to react with FeCl₂ in CH₃CN–H₂O 4 : 1 at r.t. for 2 h. Chromatographic purification of the reaction mixture afforded two major products (**5a** and **5b**, Scheme 2), whose stereostructure was identified by detailed spectroscopic investigation.

Compound **5a** showed ESI-MS molecular ions at *m/z* 373 and 375 [M+Na]⁺ (relative intensity approx. 3 : 1), an isotopic pattern suggesting the presence of a chlorine atom. This was confirmed by HR-EIMS, which indicated the molecular formula C₁₈H₃₅ClO₄, with one unsaturation degree. Since the methyl ester group is still present in compound **5a** (δ_C 174.6; δ_C 51.0, δ_H 3.72), the molecule must be acyclic (proton NMR spectrum of **5a** available as ESI[†]). Analysis of the 2D COSY and HSQC spectra of **5a** allowed us to disclose two distinct spin systems (highlighted in Fig. 5), which strictly mirrored the spin systems of dihydroplakortin, with more significant differences restricted to the “western” moiety. Within this moiety, the attachment of the chlorine atom at C13 (δ_H 4.53, δ_C 64.2) resulted from the COSY coupling of H13 with the relatively deshielded methyl protons at δ_H 1.45 (H₃14) and with the methine H8 (δ_H 1.83), this latter proton belonging to a 6-carbon linear chain (from C7 to C12). The HMBC spectrum of **5a** confirmed this assignment and allowed the complete elucidation of the planar structure of compound **5a**. The most significant



Scheme 2 Products obtained upon reaction of plakortin and dihydroplakortin with iron(II) chloride

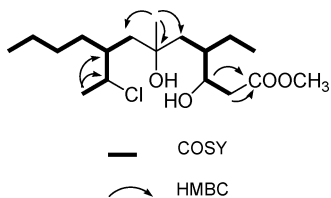


Fig. 5 COSY and key HMBC cross-peaks detected for compound **5a**.

HMBC cross-peaks are reported in Fig. 5. Elucidation of absolute configuration at the single newly created chiral center C13 was not trivial. To solve this issue, the *J*-based configuration analysis proposed by Murata for relative configurations in acyclic system was applied.²² This method is based on the combined analysis of the coupling constants $^2J_{C,H}$ (in systems $^1H-C-^{13}C-X$, related to the dihedral angle between the proton and the heteroatom), $^3J_{H,H}$ and $^3J_{C,H}$ (both related to conformational parameters through the Karplus rule). The original method was proposed for $X = OR$ but it was successively extended also to $X = Cl$ and other different electron-withdrawing groups.^{23,24} Since C13 was adjacent to the chiral carbon atom C8, and the small value of $^3J_{H8/H13}$ (1.5 Hz) indicated that a dominant rotamer (with the two protons in a *gauche* orientation) existed around the C8/C13 axis, our molecule appeared to possess all the requirements essential for application of the Murata's method.²² We qualitatively determined the four required heteronuclear coupling constants through an analysis of the phase-sensitive HMBC (PS-HMBC) spectrum and the obtained *J* data indicated a *threo* stereochemical relationship between C8 and C13 in compound **5a** (Fig. 6). Consequently, on the basis of the known *S* configuration assigned at C8 for **3**, we deduced an *R* configuration at C13 of **5a**.

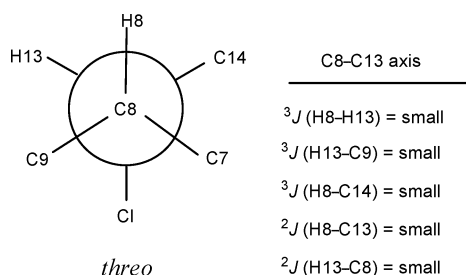


Fig. 6 Application of the Murata method to the C8–C13 axis of compound **5a**.

Small amounts of the epimer at position 13, **5b** ($C_{18}H_{35}ClO_4$ by HR-EIMS), were also obtained. This molecule was easily identified on the basis of the broad similarities among its 1H and ^{13}C NMR spectra and corresponding spectra of **5a**. The planar structure and signal assignment were then unambiguously deduced on the basis of 2H -NMR spectral (COSY, HSQC, HMBC) data. Since the small differences between the two series of NMR data are restricted to C/H resonances bordering with position 13, we confidently assigned the stereostructure of **5b** as the epimer of **5a** at the newly created chiral center C13. The reaction affording **5a** and **5b** is not stereospecific, however it produces **5a** in consistently higher amounts (about 6 : 1).

Reaction with $FeCl_2$ was then repeated for **2** in the same conditions (solv. CH_3CN-H_2O 4 : 1; r.t.; 2 h) previously employed for **3**, yielding only two major products, **6a** and **6b** (Scheme 2), in ab. 2 : 1

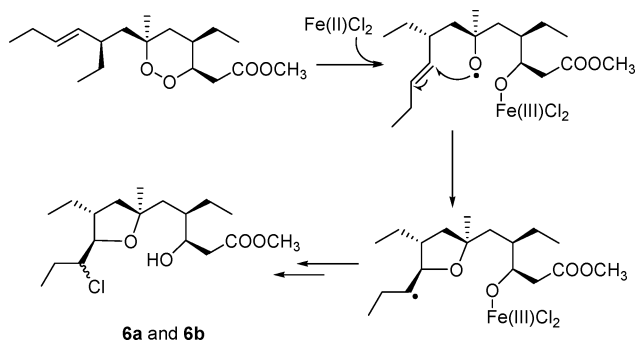
relative yields. Determination of the complete stereostructures of these products proved to be quite simple, indeed, the structure of compound **6a**, $C_{18}H_{33}ClO_4$ by HR-EIMS, was assigned on the basis of the absolute identity of its spectroscopic data ($[\alpha]_D$, 1H NMR, ^{13}C NMR) with those of plakortether C, a natural analogue of plakortin that we isolated some years ago from *Plakortis simplex* and whose complete absolute stereostructure was established (proton NMR spectrum of **6a** available as ESI†).²⁵

Compound **6b** showed the same molecular formula and very similar 1H and ^{13}C NMR spectra compared to **6a**. Investigation of the 2H -NMR spectra (COSY, HSQC, HMBC) of **6b** indicated that this molecule must possess the same planar structure of **6a**; thus, as for **3**, the reaction produced a mixture of diastereomers. Inspection of the ROESY spectrum of **6b** disclosed a *cis* relationship between H9 and H₃15, identical to that of compound **6a**. Therefore, the difference between compounds **6a** and **6b** must reside on the configuration at C10 and consequently, compound **6b** was identified as the epimer at C10 of **6a**.

3. Discussion

The above described computational and experimental investigations completely agree in suggesting the possible steps connecting the interaction of Fe(II)heme/plakortin [or Fe(II)heme/dihydroplakortin] with the death of the parasite. In addition, obtained results stimulate some interesting considerations about the mechanism of antimalarial action of plakortins and related simple 1,2-dioxanes.

The formation of the products **6a/6b** obtained upon reaction of **2** with $FeCl_2$, can be interpreted only by assuming the preferential formation of the oxygen radical at O1 (Scheme 3), in agreement with anticipation of computational calculations. In addition, the formation of O1–C9 linkage indicates that the O1 radical tends to react with the “western” side-chain double bond, giving the consequent formation of the carbon radical at C10. Interestingly, the obtainment of a single configuration at C9 suggests that the reaction proceeds through a concerted mechanism, where the following events occur in a single step: i) electron uptake from iron, ii) O1–O2 bond breaking with consequent O1 radical formation, iii) O1–C9 bonding with consequent C10 radical formation. This latter species represents the key toxic intermediate responsible for plakortin antimalarial activity and it is involved in a subsequent intermolecular reaction. These are valuable insights for the design of new derivatives since this reaction mechanism implies that



Scheme 3 Mechanism hypothesized for the formation of compounds **6a** and **6b** upon reaction of plakortin (**2**) with $FeCl_2$.

the structure must simultaneously orientate all intramolecular reaction partners in order to trigger production of the toxic carbon radical. These results are in agreement with our previous conclusions that the lower activity of plakortins compared to artemisinin could be also attributed to the marked difference in the conformational behavior exhibited by these molecules.⁸

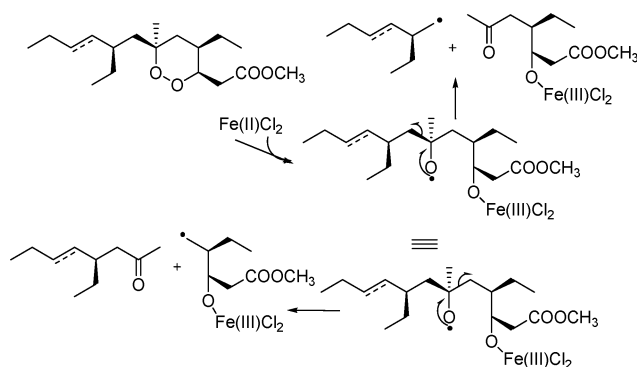
In the experimental model, the C10 carbon radical reacts to give the chlorine-linking mixture **6a/6b** (Scheme 3). The formation of this diastereomeric mixture evidenced that the chlorination was not concerted with the electron transfer reaction leading to formation of C10 radical.

Also in the case of dihydroplakortin (Scheme 4), the obtained products suggest that the endoperoxide bond cleavage produced preferentially an oxygen radical at O1. In addition, products **5a/5b** indicate a selective involvement of C13 hydrogens in the subsequent rearrangement which, most likely, takes place through a 1,5-H shift with formation of a carbon radical at that position. Then, the diastereoisomeric mixture of products **5a/5b** was formed upon chlorination at C13. As a consequence, in the case of **3**, the C13 carbon radical should be the toxic intermediate responsible for the antimalarial activity.

Data about the exact mechanism going from carbon radicals of both plakortin (at C10) and dihydroplakortin (at C13) to the corresponding chlorinated species are not available. A plausible hypothesis is a “chloro-Fenton” reaction involving direct abstraction of a chlorine atom linked at the Fe(III) center, recently proposed in a similar case.²⁶

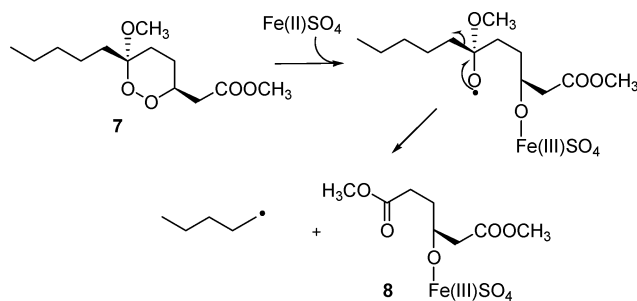
The observation of a diastereomeric mixture of chlorinated products, both for **2** and **3**, supports the availability of the formed carbon radicals (*i.e.*, C10 and C13, respectively) for intermolecular reactions. These carbon radicals may exert their toxicity through direct reaction with plasmodium biomolecules (*e.g.*, food vacuole membrane lipids, heme, protein residues, glutathione), not requiring molecular oxygen to induce the oxidative stress in the parasite. The key role of carbon radicals, available for intermolecular reactions, is also supported by the behavior of artemisinin and derivatives, where steric hindrance significantly affecting carbon radical reactivity has a negative impact on antimalarial potency.^{9,13}

Another remarkable outcome of our experiments is the complete absence (or undetectable presence) of cleavage products, upon reaction of **2** and **3** with FeCl₂. Indeed, following the mechanism of oxygen radical evolution described for artemisinin derivatives (Scheme 1),^{9,15} the formation of the carbon–carbon cleavage products depicted in Scheme 5 could be hypothesized.

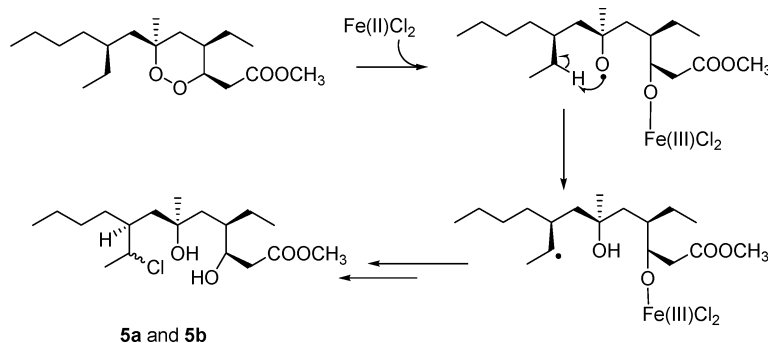


Scheme 5 Postulated mechanism for the formation of carbon–carbon cleavage products from plakortin (or dihydroplakortin).

Thus, the absence of the postulated ketone derivatives as well as of products which could derive from the rearrangement/reaction of the postulated primary carbon radicals indicated that, at least in our experimental conditions, the cleavage mechanism does not operate for **2** and **3**. In this regard, it is interesting to notice that peroxyketal derivatives, structurally related to plakortin (*e.g.* compound **7**,²⁷ Scheme 6), have been reported to produce, upon reaction in similar experimental conditions (FeSO₄ in aqueous solution), mostly cleavage products (*e.g.* **8**, Scheme 6).²⁸ Given the wide similarity between the two carbon scaffolds, the marked difference between the products obtained, upon reaction of **7** and **2** with ferrous ion, is a clear evidence that minor differences in the functionality pattern of a 1,2-dioxane (*e.g.* the presence of a peroxyketal in **7**) can result into dramatic differences in the evolution of the oxygen radicals.



Scheme 6 FeSO₄-induced cleavage of compound **7**. Data taken from ref. 27.



Scheme 4 Mechanism hypothesized for the formation of compounds **5a** and **5b** upon reaction of dihydroplakortin (**3**) with FeCl₂.

The results of our combined studies on plakortin and dihydroplakortin evidenced that plakortin alkyl chain double bond reactivity likely supports carbon radical formation, on the other hand, the weaker side-chain reactivity of dihydroplakortin is balanced by favorable conformational parameters. This accounts for the comparable antimalarial activity of the two compounds (Table 1), despite the structural differences in their alkyl chains.

The results of our investigation, in agreement with previously reported SARs,⁸ also evidenced that the ester side-chain is not directly involved in the formation of carbon radical intermediates, nevertheless, our docking results demonstrated that the presence of ester group may play a role in the interaction with iron, affecting endoperoxide approach to heme. Thus, the presence of iron-coordinating groups, other than the endoperoxide functionality, must be taken into consideration for the design of new plakortin-like antimalarials.

4. Experimental

4.1 Molecular modeling

Molecular modeling calculations were performed using SGI Origin 200 8XR12000, while molecular modeling graphics were generated on SGI Octane 2 workstations.

Compounds **2** and **3** were built using the Insight 2005 Builder module. Atomic potentials and charges were assigned using the CFF91 force field.²⁹ The conformational space of the compounds was sampled through 500 cycles of Simulated Annealing ($\epsilon = 80^{\circ}r$) by following this protocol: the system was heated up to 1000 K over 2000 fs (time step = 3.0); a temperature of 1000 K was applied to the system for 2000 fs (time step = 3.0) with the aim of surmounting torsional barriers; successively the temperature was linearly reduced to 300 K in 1000 fs (time step = 1.0). The resulting structures were subjected to energy minimization within the Insight 2005 Discover module (CFF91 force field; $\epsilon = 80^{\circ}r$) until the maximum RMS derivative was less than 0.001 kcal \AA^{-1} , using Conjugate Gradient³⁰ as the minimization algorithm. The obtained conformers were ranked by their conformational energy, torsional angles and interatomic distance values.

In order to properly analyze the electronic properties, all conformers, obtained from molecular dynamics and mechanics calculations, were subjected to a full geometry optimization by semiempirical calculations, using the QM method PM6³¹ in the Mopac2007 package³² and EF³³ (Eigenvector Following routine) as the geometry optimization algorithm. The GNORM value was set to 0.01. To reach a full geometry optimization the criteria for terminating all optimizations was increased by a factor of 100, using the keyword PRECISE. The resulting conformers were ranked by their conformational energy, torsional angles and interatomic distances values. The most stable conformers of **2** and **3** were selected for *ab initio* calculations.

4.2 *Ab initio* calculations

All the calculations were carried out using the Gaussian 03 package³⁴ using the PBE0 hybrid density functional³⁵ with Pople's basis set 6-31G(d).³⁶ After full geometry optimization, the different stationary points were characterized as minima or transition states by calculating the harmonic vibrational frequencies. Bulk

solvent effects were taken into account by the PCM,^{37,38} in which the solvent is represented by an infinite dielectric medium characterized by the relative dielectric constant of the bulk, and the UAHF radii²⁸ are used for building the effective cavity occupied by the solute in the solvent.

4.3 Docking studies

In order to find the bioactive conformation of **2** and **3**, docking studies were carried out on both compounds in complex with heme, using a docking methodology (Affinity, SA_Docking; Insight2005, Accelrys, San Diego) which considers all the systems flexible (*i.e.*, ligand and protein). Atomic potentials were assigned using the Heme29.frc,³⁹ a force field including heme parameters, while the atomic partial charges were assigned using PM6, a QM method able to parameterize the iron atom. According to the estimation of heme apparent pK_a values, calculated by using the ACD/ pK_a DB version 11.00 software (Advanced Chemistry Development Inc., Toronto, Canada), the total charge of the heme was set at 1 and the heme was considered both fully deprotonated and monoprotinated at the level of propionic moieties. Although in the subsequent dynamic docking protocol all the systems were perturbed by means of Monte Carlo and simulated annealing procedures, nevertheless the dynamic docking procedure formally requires a reasonable starting structure. As starting conformations for the ligands, all the conformers of **2** and **3** obtained from *ab initio* calculations were selected, while for the heme, the its conformation in the homology model of lanosterol 14- α -demethylase of *C. albicans* was selected.³⁹ The ligands were placed above the heme taking into account the crystal structure of a peroxo-bridged heme-copper dinuclear complex (CSD code: UKACIS).

Flexible docking was achieved using the Affinity module in the Insight 2005 suite, setting the SA_Docking procedure,⁴⁰ and using the Cell_Multipole⁴¹ method for non-bond interactions. Heme and the ligands were left free to move during the entire docking calculations with the exception of the heme pyrrolic carbons, that were fixed. A Monte Carlo/minimization approach for the random generation of a maximum of 20 acceptable ligand/heme complexes, for each compound, was used. During the first step, starting from the previously obtained roughly docked structures, the ligand was moved by a random combination of translation, rotation, and torsional changes (Flexible_Ligand option, considering all rotatable bonds) to sample both the conformational space of the ligand and its orientation with respect to the heme (MxRChange = 3 \AA ; MxAngChange = 180 $^{\circ}$). During this step, vdW and Coulombic terms were scaled to a factor of 0.1 to avoid very severe divergences in the Coulombic and vdW energies. If the energy of a complex structure resulting from random moves of the ligand was higher by the energy tolerance parameter than the energy of the last accepted structure, it was not accepted for minimization. To ensure a wide variance of the input structures to be successively minimized, an energy tolerance value of 10⁶ kcal mol⁻¹ from the previous structure has been used. After the energy minimization step (conjugate gradient; 2500 iterations; $\epsilon = 80^{\circ}r$), the Metropolis test, at a temperature of 310 K, and a structure similarity check (rms tolerance = 0.3 kcal \AA^{-1}), were applied to select the 20 acceptable structures. Each subsequent structure was generated from the last accepted structure.

All the accepted complexes resulting from the Monte Carlo/minimization approach were subjected to a molecular dynamics simulated annealing protocol, including 5 ps of a dynamic run divided in 50 stages (100 fs each) during which the temperature of the system was linearly decreased from 500 to 300 K (Verlet velocity integrator; time step = 1.0 fs). In simulated annealing, the temperature is altered in time increments from an initial temperature to a final temperature. The temperature is changed by adjusting the kinetic energy of the structure (by rescaling the velocities of the atoms). Molecular dynamics calculations were performed using a constant temperature and constant volume (NVT) statistical ensemble, and the direct velocity scaling as temperature control method (temp window = 10 K). In the first stage, initial velocities were randomly generated from Boltzmann distribution, according to the desired temperature, while during the subsequent stages initial velocities were generated from Dynamics Restart Data. A temperature of 500 K was applied with the aim of surmounting torsional barriers, thus allowing an unconstrained rearrangement of the ligand and the heme (initial vdW and Coulombic scale factors = 0.1). Successively temperature was linearly reduced to 300 K in 5 ps, and concurrently the scale factors have been similarly decreased from their initial values (0.1) to their final values (1.0). A final round of 10^4 minimization steps (conjugate gradient, $\varepsilon = 80^*r$) followed the last dynamics steps, and the minimized structures were saved in a trajectory file.

After this procedure, the resulting docked structures were ranked by their conformational energy and the geometry of endoperoxide–iron coordination bond.

The ligand–enzyme interaction energy of each complex was evaluated by calculating: i) the total energy between the ligand and the heme, using the Evaluate command in the Docking module of Insight 2005 (vdW and electrostatic energy contribution; no CUT_OFF), ii) the nonbond interaction energy between the ligand and the heme, using the Discover_3 Module of Insight2005 (vdW and electrostatic energy contribution; no CUT_OFF). The complex with the best compromise between the binding energy and the coordination geometry was selected as structure representing the most probable binding mode.

4.4 General chemical procedures

Low-resolution ESI-MS was performed on a LCQ Finnigan MAT mass spectrometer. Optical rotations (CHCl_3) were measured at 589 nm on a Perkin-Elmer 192 polarimeter equipped with a sodium lamp ($\lambda = 589$ nm) and a 10 cm microcell. ^1H (500 MHz) and ^{13}C (125 MHz) NMR spectra were measured on a Varian INOVA spectrometer. Chemical shifts were referenced to the residual solvent signal (CDCl_3 ; $\delta_{\text{H}} 7.26$, $\delta_{\text{C}} 77.0$). Homonuclear ^1H connectivities were determined using the COSY experiment. One-bond heteronuclear ^1H – ^{13}C connectivities were determined using the HSQC experiment. Two- and three-bond ^1H – ^{13}C connectivities were determined by HMBC experiments optimized for a 2J of 7 Hz. Through-space ^1H connectivities were evidenced using a ROESY experiment with a mixing time of 500 ms. Two and three bond ^1H – ^{13}C connectivities were determined by gradient 2D HMBC experiments optimized for a 2J of 9 Hz. Phase sensitive (PS)-HMBC spectra were recorded with the delay set at 40 ms and a data size of 2 K (F_2) \times 128 (F_1) points. Reactions were monitored by TLC on Merck 60 F₂₅₄ (0.25 mm) plates, that were

visualized by UV inspection and/or staining with 5% H_2SO_4 in ethanol and heating. A Knauer HPLC apparatus equipped with refraction index detector was used to purify and assess purity (>95%) of all final products. LUNA (normal phase) (Phenomenex) columns were used, with elution with EtOAc–*n*-hexane mixtures and 0.7 mL min^{−1} as the flow rate.

4.5 Reaction of dihydroplakortin (3) with FeCl_2

Dihydroplakortin (**3**, 25.0 mg, 0.080 mmol) was dissolved in CH_3CN – H_2O 4:1 (5 mL) and freshly purchased $\text{FeCl}_2 \cdot 4\text{H}_2\text{O}$ (78 mg, 0.40 mmol) was added. The reaction mixture was left under stirring at room temperature for 2 h. Light was excluded from the reaction. Then the obtained mixture was partitioned between water and EtOAc. The organic phase, dried over Na_2SO_4 , was purified by HPLC (SI60 *n*-hexane–EtOAc 85:15) affording compounds **5a** (15.0 mg, 0.040 mmol, 50%) and **5b** (2.5 mg, 0.0067 mmol, 8%) in the pure state. Compound **5a**. Colorless oil. $[\alpha]_{\text{D}}^{25} +35$ (*c* 0.10 in CHCl_3). ^1H NMR (CDCl_3 , 500 MHz): δ 4.53 (H13, dq, *J* 6.90, 1.5); 4.19 (H3, m); 3.72 (OMe, s); 2.56 (H2a, dd, *J* 16.4, 10.5); 2.37 (H2b, dd, *J* 16.4, 10.5); 1.97 (H4, m); 1.83 (H8, m); 1.77 (H7a, dd, *J* 14.2, 5.6); 1.67 (H5a, dd, *J* 14.4, 9.0); 1.45 (H3-14, d, *J* 6.90); 1.39–1.31 (H2-9, H2-10, H2-11, m) 1.31 (H7b, overlapped); 1.29 (H5b, overlapped); 1.27 (H16a, overlapped); 1.17 (H3-15, s); 1.16 (H16b, overlapped); 0.90 (H3-12, t, *J* 7.2). ^{13}C NMR (CDCl_3 , 125 MHz): δ 174.6 (C1); 71.9 (C6); 70.8 (C3); 64.2 (C13); 51.0 (OMe); 45.1 (C7); 42.8 (C5); 41.3 (C8); 40.1 (C4); 37.0 (C2); 31.2 (C9); 30.3 (C10); 26.9 (C17); 26.4 (C15); 23.4 (C11); 23.0 (C14); 13.4 (C12); 12.9 (C18). ESI-MS: *m/z* 373 and 375 (3:1) [*M* + *Na*]⁺. EIMS: *m/z* 350 and 352 (*M*). HR-EIMS: *m/z* 350.2229, calcd. for $\text{C}_{18}\text{H}_{35}^{35}\text{ClO}_4$ *m/z* 350.2224. Compound **5b**. Colorless oil. $[\alpha]_{\text{D}}^{25} +22$ (*c* 0.10 in CHCl_3). ^1H NMR (CDCl_3 , 500 MHz): δ 4.58 (H13, m); 4.19 (H3, m); 3.72 (OMe, s); 2.56 (H2a, dd, *J* 16.4, 10.5); 2.37 (H2b, dd, *J* 16.4, 10.5); 1.97 (H4, m); 1.83 (H8, m); 1.77 (H7, dd, *J* 14.2, 5.6); 1.67 (H5a, dd, *J* 14.4, 9.0); 1.37 (H3-14, d, *J* 7.2); 1.39–1.31 (H2-9, H2-10, H2-11) 1.31 (H7b, overlapped); 1.29 (H5b, overlapped); 1.27 (H16a, overlapped); 1.17 (H3-15, s); 1.16 (H16b, overlapped); 0.90 (H3-12, t, *J* 7.2). ESI-MS: *m/z* 373 and 375 (3:1) [*M* + *Na*]⁺. EIMS: *m/z* 350 and 352 (*M*). HR-EIMS: *m/z* 350.2217, calcd. for $\text{C}_{18}\text{H}_{35}^{35}\text{ClO}_4$ *m/z* 350.2224.

4.6 Reaction of plakortin (2) with FeCl_2

Plakortin (**2**, 50.2 mg, 0.16 mmol) was dissolved in CH_3CN – H_2O 4:1 (8 mL) and $\text{FeCl}_2 \cdot 4\text{H}_2\text{O}$ (155 mg, 0.80 mmol) was added. The reaction mixture was left under stirring at room temperature for 2 h. Light was excluded from the reaction. Then the obtained mixture was partitioned between water and EtOAc. The organic phase, dried over Na_2SO_4 , was purified by HPLC (SI60 *n*-hexane–EtOAc 9:1) affording compounds **6a** (27.0 mg, 0.077 mmol, 48%) and **6b** (13 mg, 0.037 mmol, 23%) in the pure state. Compound **6a**. Colorless oil. $[\alpha]_{\text{D}}^{25} -6$ (*c* 0.10 in CHCl_3). ESI-MS: *m/z* 371 and 373 (3:1) [*M* + *Na*]⁺. HR-EIMS: *m/z* 348.2059, calcd. for $\text{C}_{18}\text{H}_{33}^{35}\text{ClO}_4$ *m/z* 348.2067. ^1H and ^{13}C NMR: see data reported in ref. 25. Compound **6b**. $[\alpha]_{\text{D}}^{25} -13$ (*c* 0.10 in CHCl_3). ^1H NMR (CDCl_3 , 500 MHz): δ 4.32 (H3, m); 3.91 (H10, m); 3.81 (H9, m); 3.70 (OMe, s); 2.66 (H2a, dd, *J* 16.4, 10.5); 2.36 (H2b, dd, *J* 16.4, 10.5); 2.22 (H8, m); 2.06 (H7a, m); 1.87 (H2-11, m); 1.78 (H4, m); 1.69 (H5a, dd, *J* 14.0, 9.0); 1.55 (H7b, overlapped); 1.51 (H5b,

overlapped); 1.39 (H16a, m); 1.28 (H₃15, s); 1.25 (H₂13, m); 1.20 (H16b, m); 1.06 (H₃12, t, *J* 7.2); 0.94 (H₃14, t, *J* 7.2); 0.92 (H₃17, d, *J* 6.90). ESI-MS: *m/z* 371 and 373 (3 : 1) [M + Na]⁺. HR-EIMS: *m/z* 348.2070, calcd. for C₁₈H₃₃³⁵ClO₄ *m/z* 348.2067.

5. Conclusions

Throughout this paper, computational calculations and experimental models concurred to clarify the antimalarial mechanism of action of plakortins, based on the interaction of their endoperoxide bond with the Fe(II) belonging to the heme molecule. This mechanism involves the formation of an oxygen radical and its “through-space” rearrangement to give a carbon radical centered on the “western” alkyl side-chain, which is the toxic intermediate able to directly react with parasite biomolecules. Moreover, the following minimal structural requirements, necessary for the activity of this class of antimalarial agents, were identified (Fig. 7): i) a 1,2-dioxane ring able to react with Fe(II) species through its endoperoxide group and to form an oxygen radical; ii) a side-chain bearing possible partners for a “through-space” intramolecular radical shift from the oxygen to a carbon atom, iii) a conformational preference for the conformer which allows the correct orientation of all the intramolecular reaction partners, and iv) the formation of a carbon radical amenable of intermolecular reactions. On these bases, a 1,2-dioxane ring side-chain combining good reactivity (such as in plakortin) with favorable conformational preference (such as in dihydroplakortin) should improve antimalarial activity. The synthesis of 1,2-dioxanes, rationally designed on the basis of the above concepts, is in progress in our labs.

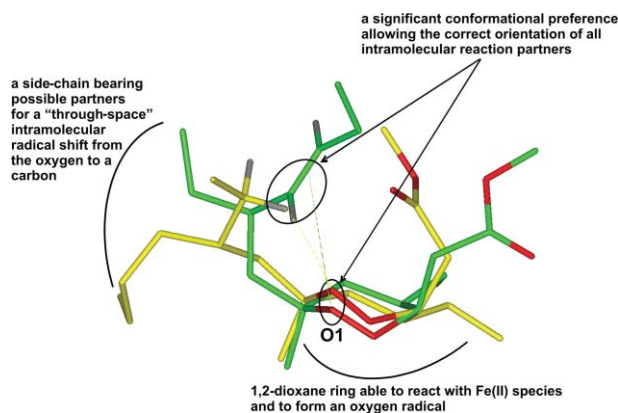


Fig. 7 A view of the structural requirements necessary for the antimalarial activity of 1,2-dioxanes.

Acknowledgements

This work is the result of research supported by the European Community (ANTIMAL project–EU contract LSHP-CT-2005-018834) and by Regione Campania (Italy), (Legge Regionale 5/02, Annualità 2007). Mass and NMR spectra were recorded at the “Centro di Servizio Interdipartimentale di Analisi Strumentale”, Università di Napoli “Federico II”. The assistance of the staff is acknowledged. Marco Persico, Italian Malaria Network, was funded by Compagnia di San Paolo, Torino, Italy.

References

- 1 R. W. Snow, C. A. Guerra, A. M. Noor, H. Y. Myint and S. I. Hay, *Nature*, 2005, **434**, 214–217.
- 2 <http://www.who.int>.
- 3 N. J. White, *Science*, 2008, **320**, 330–334, and references cited therein.
- 4 E. E. Korshin, R. Hoos, A. M. Szpilman, L. Konstantinovski, G. H. Posner and M. D. Bachi, *Tetrahedron*, 2002, **58**, 2449–2469.
- 5 F. Cafieri, E. Fattorusso, O. Taglialatela-Scafati and A. Ianaro, *Tetrahedron*, 1999, **55**, 7045–7056.
- 6 E. Fattorusso, S. Parapini, C. Campagnuolo, N. Basilico, O. Taglialatela-Scafati and D. Taramelli, *J. Antimicrob. Chemother.*, 2002, **50**, 883–888.
- 7 C. Campagnuolo, E. Fattorusso, A. Romano, O. Taglialatela-Scafati, N. Basilico, S. Parapini and D. Taramelli, *Eur. J. Org. Chem.*, 2005, 5077–5083.
- 8 C. Fattorusso, G. Campiani, B. Catalanotti, M. Persico, N. Basilico, S. Parapini, D. Taramelli, C. Campagnuolo, E. Fattorusso, A. Romano and O. Taglialatela-Scafati, *J. Med. Chem.*, 2006, **49**, 7088–7094.
- 9 C. W. Jefford, *Curr. Med. Chem.*, 2001, **15**, 1803–1826 and references cited therein; C. W. Jefford, *Drug Discovery Today*, 2007, **12**, 487–495; A. Robert, F. Benoit-Vical, O. Dechy-Cabaret and B. Meunier, *Pure Appl. Chem.*, 2001, **73**, 1173–1188; Y. Tang, Y. Dong and J. L. Vennerstrom, *Med. Res. Rev.*, 2004, **24**, 425–448.
- 10 (a) R. Kannan, D. Sahal and V. S. Chauhan, *Chem. Biol.*, 2002, **9**, 321–332; (b) K. Becker, L. Tilley, J. L. Vennerstrom, D. Roberts, S. Rogerson and H. Ginsburg, *Int. J. Parasitol.*, 2004, **34**, 163–89.
- 11 P. M. O'Neill and G. H. Posner, *J. Med. Chem.*, 2004, **47**, 2945–2964.
- 12 C. Arantes, M. T. de Araujo, A. G. Taranto and J. W. D. Carneiro, *Int. J. Quantum Chem.*, 2005, **103**, 749–762; M. G. B. Drew, J. Metcalfe, M. J. Dascombe and F. M. D. Ismail, *THEOCHEM*, 2007, **823**, 34–46.
- 13 G. H. Posner, D. Wang, J. N. Cumming, C. H. Oh, A. N. French, A. L. Bodley and T. A. Shapiro, *J. Med. Chem.*, 1995, **38**, 2273–2275; G. H. Posner, C. H. Oh, D. Wang, L. Gerena, W. K. Milhous, S. R. Meshnick and W. Asawamahasadka, *J. Med. Chem.*, 1994, **37**, 1256–1258.
- 14 M. Kawanishi, N. Kotoku, S. Itagaki, T. Horii and M. Kobayashi, *Bioorg. Med. Chem.*, 2004, **12**, 5297–5307.
- 15 A. Robert, O. Dechy-Cabaret, J. Cazelles and B. Meunier, *Acc. Chem. Res.*, 2002, **35**, 167–174.
- 16 D. C. Magri and M. S. Workentin, *Chem.–Eur. J.*, 2008, **14**, 1698–1709.
- 17 R. L. Donkers and M. S. Workentin, *J. Phys. Chem. B*, 1998, **102**, 4061–4063; R. L. Donkers and M. S. Workentin, *J. Am. Chem. Soc.*, 2004, **126**, 1688–1698.
- 18 J.-F. Hu, H.-F. Gao, M. Kelly and M. T. Hamann, *Tetrahedron*, 2001, **57**, 9379–9383.
- 19 R. K. Haynes and S. C. Vonwiller, *Tetrahedron Lett.*, 1996, **37**, 257–260.
- 20 D. J. Creek, F. C. K. Chiu, R. J. Prankerd, S. A. Charman and W. N. Charman, *J. Pharm. Sci.*, 2005, **94**, 1820–1829.
- 21 G. H. Posner and H. Dowd, *Heterocycles*, 1998, **47**, 643–646.
- 22 N. Matsumori, D. Kaneno, M. Murata, H. Nakamura and K. Tachibana, *J. Org. Chem.*, 1999, **64**, 866–876.
- 23 P. Ciminiello, E. Fattorusso, M. Forino and R. Poletti, *J. Org. Chem.*, 2001, **66**, 578–582.
- 24 C. Campagnuolo, C. Fattorusso, E. Fattorusso, A. Ianaro, B. Pisano and O. Taglialatela-Scafati, *Org. Lett.*, 2003, **5**, 673–676.
- 25 C. Campagnuolo, C. Fattorusso, E. Fattorusso, A. Ianaro, B. Pisano and O. Taglialatela-Scafati, *Eur. J. Org. Chem.*, 2002, 61–69.
- 26 D. S. Dalisay, T. Quach, G. N. Nicholas and T. F. Molinski, *Angew. Chem., Int. Ed.*, 2009, **48**, 4367–4371.
- 27 N. Murakami, M. Kawanishi, S. Itagaki, T. Horii and M. Kobayashi, *Bioorg. Med. Chem. Lett.*, 2002, **12**, 69–72.
- 28 N. Murakami, M. Kawanishi, S. Itagaki, T. Horii and M. Kobayashi, *Bioorg. Med. Chem. Lett.*, 2004, **14**, 3513–3516.
- 29 J. R. Maple, M. J. Hwang, T. P. Stockfish, U. Dinur, M. Waldman, C. S. Ewig and A. T. Hagler, *J. Comput. Chem.*, 1994, **15**, 162–182.
- 30 R. Fletcher, In *Practical Methods of Optimization*, John Wiley & Sons, New York, 1980, Vol.1.
- 31 MOPAC2007, James J. P. Stewart, *Stewart Computational Chemistry*, Colorado Springs, CO, USA, [HTTP://OpenMOPAC.net](http://OpenMOPAC.net) 2007.
- 32 J. J. P. Stewart, *J. Mol. Model.*, 2007, **13**, 1173–1213.
- 33 J. Baker, *J. Comput. Chem.*, 1986, **7**, 385–395.
- 34 M. J. Frisch, G. W. Trucks, H. B. Schlegel, G. E. Scuseria, M. A. Robb, J. R. Cheeseman, J. A. Montgomery, Jr., T. Vreven, K. N. Kudin, J. C. Burant, J. M. Millam, S. S. Iyengar, J. Tomasi, V. Barone, B. Mennucci, M. Cossi, G. Scalmani, N. Rega, G. A. Petersson, H. Nakatsuji, M.

- Hada, M. Ehara, K. Toyota, R. Fukuda, J. Hasegawa, M. Ishida, T. Nakajima, Y. Honda, O. Kitao, H. Nakai, M. Klene, X. Li, J. E. Knox, H. P. Hratchian, J. B. Cross, V. Bakken, C. Adamo, J. Jaramillo, R. Gomperts, R. E. Stratmann, O. Yazyev, A. J. Austin, R. Cammi, C. Pomelli, J. Ochterski, P. Y. Ayala, K. Morokuma, G. A. Voth, P. Salvador, J. J. Dannenberg, V. G. Zakrzewski, S. Dapprich, A. D. Daniels, M. C. Strain, O. Farkas, D. K. Malick, A. D. Rabuck, K. Raghavachari, J. B. Foresman, J. V. Ortiz, Q. Cui, A. G. Baboul, S. Clifford, J. Cioslowski, B. B. Stefanov, G. Liu, A. Liashenko, P. Piskorz, I. Komaromi, R. L. Martin, D. J. Fox, T. Keith, M. A. Al-Laham, C. Y. Peng, A. Nanayakkara, M. Challacombe, P. M. W. Gill, B. G. Johnson, W. Chen, M. W. Wong, C. Gonzalez and J. A. Pople, *GAUSSIAN 03 (Revision C.02)*, Gaussian, Inc., Wallingford, CT, 2004.
- 35 C. Adamo and V. Barone, *J. Chem. Phys.*, 1999, **110**, 6158.
- 36 J. B. Foresman, A. E. Frisch, *Exploring Chemistry with Electronic Structure Methods*, 2nd Ed., Gaussian Inc., Pittsburg, PA, 1996.
- 37 M. Cossi, G. Scalmani, N. Rega and V. Barone, *J. Chem. Phys.*, 2002, **117**, 43–54.
- 38 G. Scalmani, V. Barone, K. N. Kudin, C. S. Pomelli, G. E. Scuseria and M. Frisch, *J. Theor. Chem. Acc.*, 2004, **111**, 90–100.
- 39 H. D. Holtje and C. Fattorusso, *Pharm. Acta Helv.*, 1998, **72**, 271–277.
- 40 H. Senderowitz, F. Guarnieri and W. C. Still, *J. Am. Chem. Soc.*, 1995, **117**, 8211–8219.
- 41 H. Q. Ding, N. Karasawa and W. A. III Goddard, *J. Chem. Phys.*, 1992, **97**, 4309–4315.